61

Architectural Symmetry Detection from 3D Urban Point Clouds: A Derivative-Free Optimization (DFO) Approach

Fan Xue, Ke Chen, and Weisheng Lu

Abstract

Symmetry is a fundamental phenomenon in not only nature and science but also cities and architectures. Architectural symmetry detection (ASD) from 3D urban point clouds is an essential step in understanding the architectures as well as creating a semantic city/building information model (CIM/BIM) to enable various applications for a smart and resilient future. However, manual segmentation and recognition of 3D urban point clouds are too time-consuming, tedious, and costly, and automatic ASD is very challenging. This paper presents a derivative-free optimization (DFO) approach for automatic ASD from 3D urban point clouds. In this paper, we formulate the problem of ASD as a nonlinear optimization problem by extending the mathematical definition of geometric symmetry with architectural styles. We develop a 'divide-and-detect' process to detect the symmetry hierarchy based on the formulation and apply the state-of-the-art DFO algorithms. A pilot study was conducted on a case of the rooftop of a neoclassical building. The proposed approach detected the global reflection from 1.4 million points in 23.5 s, and the whole symmetry hierarchy of reflections in about ten minutes. The detected symmetry hierarchy was applied to a regularity-based rooftop modeling method. The contribution of this paper is twofold. First, this paper exposes the problem of ASD to many mathematical methods through an innovative problem formulation. Secondly, the proposed DFO approach is accurate, efficient, and capable of processing large-scale 3D urban point clouds for semantic CIMs/BIMs.

Keywords

Symmetry detection • Architectural symmetry • Derivative-free optimization (DFO) • Point cloud • Semantic enrichment • Urban semantics • City information model (CIM) • Building information model (BIM)

61.1 Introduction

From quarks to animals to galaxies, symmetry is a fundamental phenomenon in nature and science. The presence of various symmetries makes an impact on not only our perceptions and recognition but also our understandings, responses, and artifacts [1]. In architecture, symmetry always finds its fundamental position across eras, continents, and cultures [2], in examples including the Parthenon of Greece, the Great Wall of China, the Taj Mahal of India, the Sydney Opera House, and 'The Gherkin' in London. Types of architectural symmetries include reflection, translation, rotation, uniform scaling, and their combinations. Architectural symmetries are not accidental but often result from considerations of function, mechanics, economics, manufacture, and aesthetics [3], e.g., for cleaner massive prefabrication and better buildability.

A semantic *city/building information model* (CIM/BIM) of these artificial architectures can enable various applications, such as architectural design, computer vision, construction management, heritage conservation, for a smart and resilient future of cities [4, 5]. Nowadays, 3D point cloud is a fashionable, affordable, and accurate data source of CIM/BIM [5]. *Architectural symmetry detection* (ASD) that reveals geometric fundamentals is an essential step in understanding the point

F. Xue (✉) · K. Chen · W. Lu
University of Hong Kong, Pokfulam, Hong Kong SAR
e-mail: xuef@hku.hk

I. Mutis and T. Hartmann (eds.), *Advances in Informatics and Computing in Civil and Construction Engineering*,
https://doi.org/10.1007/978-3-030-00220-6_61

clouds of architectures. However, many existing methods for processing point clouds to CIM/BIM fail to utilize ASD in enriching the semantic information (e.g., in surface optimization and component determination) and the overall hierarchy. As a result, the resulting CIM/BIM is often inaccurate, semantically impoverished, and unrecognizable by computers [6], e.g., symmetric beams or windows often become position and size-asymmetric in models. One reason for the absence of ASD in the methods is that automatic ASD remains very challenging, particularly in large-scale point clouds [7].

Derivative-free optimization (DFO) is a class of nonlinear optimization in mathematics and computer science [8]. It is well-known that the derivatives of a function contain information vital to finding the best values in mathematical problems. However, in many real-world complicated science and engineering problems, such as predicting protein folding, optimizing aircraft wings, as well as ASD, the derivatives the objective functions are often unavailable, unreliable, or impractical to obtain [9, 10]. DFO algorithms have shown successful records to carry out optimization under such circumstances [8, 9]. Examples of DFO applications are *general pattern search* for protein structure prediction [11] and *covariance matrix adaptation evolution strategy* (CMA-ES) [12] for as-built BIM generation from 2D images and 3D point clouds [10, 13].

This paper aims to apply state-of-the-art DFO algorithms to the problem of ASD from 3D urban point clouds. We first formulate the problem of ASD of a single symmetry to a nonlinear optimization problem by extending the definition of general symmetries. The symmetry hierarchies, including all the global and local symmetries and their relationships in a 3D urban point cloud, can thereafter be established in a ‘divide-and-detect’ process. Then, we apply a well-known DFO algorithm CMA-ES (see [12]) to the formulated problems to detect the symmetries and the symmetry hierarchies automatically. As far as is concerned, this paper is the first attempt of applying up-to-date DFO algorithms, such as CMA-ES, to the problem of ASD from 3D urban point clouds.

The remainder of the paper is structured into four sections. Section 61.2 revisits the related methods in the literature. Section 61.3 presents the proposed DFO approach. Section 61.4 describes the experimental tests on a pilot case of a dense point cloud. Conclusion and recommendations for future research are given in Sect. 61.5.

61.2 Background

61.2.1 Symmetry

In geometry and group theory, symmetry is an affine transformation that preserves points, straight lines, and planes on the 3D Euclidean space $\mathbb{R}^3$. Symmetry detection is the process of finding the symmetry group G of a geometric object [14], e.g., a 3D point cloud $\mathcal{C}$ in this research:

$$\begin{aligned} G &= \langle \mathcal{T}, \circ \rangle, \\ \mathcal{T} &= \left\{ T | T(\mathcal{C}) = \mathcal{C}, T \text{ is affine on } \mathbb{R}^3 \right\}, \\ \mathcal{C} &= \{p_1, p_2, \ldots, p_n\} \subset \mathbb{R}^3, n > 0, \end{aligned} \tag{61.1}$$

where $\mathcal{T}$ is the set of all global symmetries, $\circ$ is the function composition defined on $\mathcal{T}$, i.e., $(g \circ f)(x) = g(f(x))$, and n is the cardinality (number of points) of $\mathcal{C}$. An affine transformation T is called a *global symmetry* if $T(\mathcal{C}) = \mathcal{C}$ [15], i.e., a global symmetry keeps $\mathcal{C}$ invariant as a whole while permuting its parts. Alternatively, T is called *local* (or *partial*) if $\exists \mathcal{C}' \subset \mathcal{C}$ such that $T(\mathcal{C})' = \mathcal{C}'$. Usually, the point cloud of a real object inevitably has instrumental, environmental, and calibration errors. Thus, the ideal global (or local) symmetry condition is often approximately relaxed to some quantitative descriptors [16, 17], such as:

$$\text{PCR} = \frac{1}{n} |T(\mathcal{C}) \cap \mathcal{C}| > 1 - \varepsilon, \tag{61.2}$$

$$\text{MSE} = \frac{1}{n} \sum_{p \in \mathcal{C}} \|T(p) - N(T(p), \mathcal{C})\|^2 < \varepsilon d^2, \tag{61.3}$$

where $0 \le \varepsilon \ll 1$ is a small threshold of error tolerance, d is the diagonal of $\mathcal{C}$, and $N(T(p), \mathcal{C})$ denotes the nearest point to the transformed point $T(p)$ in $\mathcal{C}$. A high *point correspondence ratio* (PCR) in Eq. (61.2) means that almost all points still belong to $\mathcal{C}$ after transformation T; Eq. (61.3) is the *mean square error* (MSE).

61.2.2 Symmetry Detection Methods

Researchers have developed different approaches for detecting general symmetries, including architectural symmetries, from 3D point clouds. These approaches can be broadly categorized by their methodology into three types, i.e., (i) pairwise voting-clustering based on *all* pairwise correspondences, (ii) heuristic feature matching based on heuristic (*a priori* or trained) rules, and (iii) parameter optimization based on optimization models over the parameter space.

Pairwise voting-clustering approaches are primarily based on Eq. (61.2). The core technique is the collection of *votes* for symmetry parameters in a Hough-like transform parameter space [15]. There are $n(n-1)/2$ pairwise correspondences between n points. Each correspondence 'votes' for a grid in the parameter space. The most voted grids represent the approximate parameters of the symmetries. The correspondence can be between 3D points for architectural models and symmetrization-based design [15, 16] and other geometry such as wavelet convolution [18]. However, voting-clustering approaches have limitations in processing urban point clouds, e.g., the inherited bias and proneness to the noise of the Hough-like transform [19] and ineffective recognition of local symmetries due to loss of correlation information during voting [21].

Heuristic feature matching approaches involve matching a collection of local geometric features. A feature such as a line, plane, or sphere can infer the locations and tilts of the dual symmetries, e.g., a planar rectangle naturally has two reflection symmetries. Examples of approaches include iterative closest points, boundary-tracing, matching of feature points, feature lines, and their repetitive patterns, e.g., [20, 21]. The most popular methods in this category are the variants of *random sample consensus* (RANSAC) for detecting planes, spheres, and other pre-defined features [22]. Some variants (e.g., RAPter [23]) have considered preliminary regularities for buildings, e.g., emphasizing the angles of 90 and 60 between adjacent planes to improve the results of RANSAC. However, feature matching approaches often have inevitable errors inherited from the feature detection process [22] and rely heavily on a priori rules of the point clouds and availability of an abundance of suitable and regular features [24].

Parameter optimization approaches, in contrast, focus on optimizing the parametric symmetries (e.g., the location and tilt of a reflection axis) for a satisfactory condition (see Eqs. 61.2 and 61.3). Early work in this category began with finding symmetries from 2D images, e.g., using eigenvectors of the similarity matrix [25]. In processing 3D models and point clouds to detect the symmetries and symmetry group, [17] exploited *fast Fourier transform* (FFT) and formalize the optimal axis of rotational symmetry; [26] presented a parameter optimization method for non-rigid 3D objects in general. In fact, some advanced feature matching methods, e.g., RAPter [23], also partially incorporate parameter optimization to take advantage of modern mathematical methods, though the parameters are strictly confined to the matching results of the prerequisite features.

In summary, parameter optimization approaches can detect all types of symmetries in satisfactory conditions in reasonable time. However, the optimization problem can become very complicated and expensive (time-consuming) in the dense point clouds (e.g., $n > 10^6$) of real architectures; as a result, many derivative-based mathematical methods cannot be implemented. This dilemma has given rise to attempts to develop a DFO approach in this paper.

61.3 Methodology

The set $\mathcal{T}_A$ of all architectural symmetries, as a subset of $\mathcal{T}$, can be defined on Eq. (61.1) and the style A of a known architecture:

$$\begin{aligned} &\mathcal{T}_A = \left\{T|\mathcal{A}(T) = \mathcal{A}_g(T) + \mathcal{A}_t(T) < \varepsilon_A, T \in \mathcal{T}\right\} \subseteq \mathcal{T}, \\ &\mathcal{A}_g(T) \geq 0, \\ &\mathcal{A}_t(T) \geq 0, \end{aligned} \tag{61.4}$$

where $\mathcal{A}_g$ measures the violations of the geometric regularity defined in the architectural style A, $\mathcal{A}_t$ measures the violations of the defined topology, and ε_A represents a small threshold of error tolerance. The global and local architectural symmetries can thereafter be similarly defined. For each symmetry, the problem of ASD can thus be formalized as a general form of nonlinear optimization with a weighted sum objective function:

$$
\begin{array}{lll}
min & f(x) = f_{\mathcal{C}}(x) + w\mathcal{A}(x) & \\
s.t. & x = \{x_1, x_2, \ldots, x_m\} \in \mathbb{R}^m, & \\
 & f_{\mathcal{C}} : \mathbb{R}^m \mapsto \mathbb{R}^+ \cup \{0\}, & \text{see Eq.(61.2–61.3)}, \\
 & \mathcal{A} : \mathbb{R}^m \mapsto \mathbb{R}^+ \cup \{0\}, & \text{see Eq.(61.4)}, \\
 & w \in \mathbb{R}^+ \cup \{0\}, &
\end{array}
\tag{61.5}
$$

where f is the objective function comprising of the penalty $f_{\mathcal{C}}(x)$ from the point cloud and $\mathcal{A}(x)$ from the architectural style, x a parametric transformation with m parameters, ω is the relative weight of $\mathcal{A}$. In Eq. (61.5), the violations of the soft constraints of the architectural style are converted to a weighted penalty. Equation (61.5) is general and can be applied to all architectural symmetries, such as reflection, translation, rotation, uniform scaling, and their combinations.

Because Eq. (61.5) only formulates the detection of one single symmetry, DFO algorithms must solve separately to obtain the optimal symmetries for each type of global symmetries such as reflection, rotation, translation, and scaling. The local symmetries can be detected in a 'divide-and-detect' process as follows. Every newly found symmetry splits its input $\mathcal{C}_{\text{input}}$ into three parts: the source $\mathcal{C}_{\text{src}}$ of correspondence, the destination $\mathcal{C}_{\text{dest}}$, and the non-corresponded remaining points $\mathcal{C}_{\text{rem}}$. With the formulation (Eq. 61.5) and DFO algorithms, the ASD can continue on each part by substituting $\mathcal{C}_{\text{input}}$ with $\mathcal{C}_{\text{src}}, \mathcal{C}_{\text{dest}}$, and $\mathcal{C}_{\text{rem}}$, respectively. This 'divide-and-detect' process ceases when a termination criterion, such as a maximum level or too small fragments, is met. All the detected architectural symmetries can form a family of symmetry hierarchies according to the relationships between the parts of cloud $\mathcal{C}$.

61.4 Experimental Results on a Pilot Case

A pilot study was conducted to find the reflection symmetries of a university building. The Hung Hing Ying Building at the University of Hong Kong is a two-storey neoclassical redbrick building (see Fig. 61.1a). The authors took a series of 250 aerial photos with a drone (model: DJI Inspire 1) (see Fig. 61.1b) and constructed a dense cloud of 1, 413, 211 points (over 2, 000 points/m^2) of the rooftop from the photos using the photogrammetry function provided by Autodesk ReCap 360 (see Fig. 61.1c). According to neoclassicism, we assumed the planes of the reflections on rooftops (i) must be perfectly vertical on the rooftop and (ii) prefer perpendicularity and parallelity of geometric regularity with other reflections. We defined the parameters of the vertical plane of a 3D reflection as a 2D line on the horizontal polar coordinate system L (see [16]), so that each (ρ, φ) on L represents a plane with a distance $\rho \geq 0$ to the pole O and an angle $\varphi \in (-\pi, \pi]$ of the heading direction. In fact in geometry, the point (ρ, φ) is the foot of the perpendicular from the pole O to the reflection axis on L. Due to the assumption (i), we can reduce the computational load of verifying f by partitioning the whole cloud $\mathcal{C}$ into 177 horizontal slices ($\mathcal{C}_1, \mathcal{C}_2, \ldots, \mathcal{C}_{177}$, height = 0.05 m), as shown in Fig. 61.1d.

We then formulated a nonlinear optimization problem for the reflection symmetries based on the general form of Eq. (61.5):

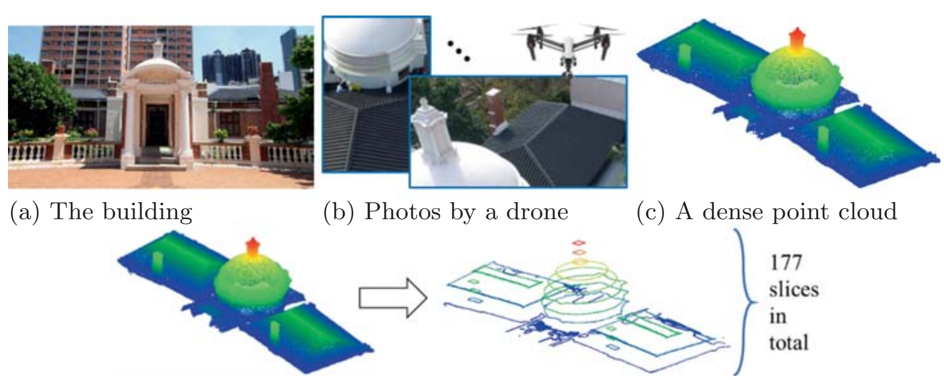

(a) The building (b) Photos by a drone (c) A dense point cloud

(d) The 177 horizontal slices for fast evaluating reflections

Fig. 61.1 A pilot case: The Hung Hing Ying building at the University of Hong Kong

$$\begin{aligned} min \quad & f(x) = f_{\mathcal{C}}(x) + 10\mathcal{A}(x) \\ s.t. \quad & x = \{\rho, \varphi\}, \\ & \rho \in \mathbb{R}^+ \cup \{0\}, \varphi \in (-\pi, \pi], \\ & f_{\mathcal{C}}(x) = \tfrac{1}{n}\sum_{i=1}^{177} |\mathcal{C}_i| \mathrm{MSE}_{\mathcal{C}_i}(x), \\ & \mathcal{A}(x) = min\_radius\_to\_perp\_or\_para(x), \end{aligned} \tag{61.6}$$

where x represents a possible vertical plane of reflection axis, $|\mathcal{C}_i|$ stands for the cardinality of $\mathcal{C}_i$, $f_{\mathcal{C}}$ is MSE (Eq. 61.3), $\mathcal{A}$ measures the minimum angular error (in radian) to the perpendicularity or parallelity against the parent symmetry, and the relative weight ω was set to 10 (e.g., a penalty $\mathcal{A}$ = 0.01 in architectural style was amplified to 0.1 in f).

We applied a C++ version of CMA-ES (*libcmaes*, version 0.9.5), a well-known DFO algorithm, to solve the formulated Eq. (61.6). The tests were conducted on a workstation (Intel Xeon E5-2690 v4 2.6 GHz, 64 GB memory, Ubuntu 16.04, single-threading), with the *point cloud library* (version 1.8.1) and *fast library for approximate nearest neighbor* (FLANN, version 1.8.4) for efficient point cloud processing. We set the number of iterations of CMA-ES to 200 and other parameters to default. Figure 61.2 shows the process of detecting the global reflection symmetry, where the objective value quickly descended from over 18 to less than 0.1 in about a minute. In the viewport of parameter space, ρ and φ quickly converged to the most voted (dark color) grid; while in the point cloud viewport, the optimal global reflection symmetry was found by CMA-ES in less than 100 s, as shown in Fig. 61.2. The time was furthermore reduced to 23.5 s on the test machine by enabling multi-threading parallel computing.

The proposed DFO approach was compared with a point-based pairwise voting-clustering [16] and a wavelet convolution-based voting method [18]. The feature matching methods were not included due to the error-prone feature detection in uncontrolled real-world scenes [22]. The feature matching Table 61.1 lists the comparisons, including PCR (Eq. 61.2), MSE (Eq. 61.3), plane equation, and computational time, of the three methods on the pilot case. According to the PCR and MSE, one can confirm the success of finding the target reflection, and evaluate the performances of different methods. The proposed DFO approach won in both accuracy (PCR = 93.7%, MSE = 0.086 m^2) and efficiency (98.7 s), while the point-based voting-clustering found a slightly less accurate and efficient result (PCR = 90.7%, MSE = 0.091 m^2, in 140.7 s), and the wavelet convolution-based voting was only with local symmetries.

The ‘divide-and-detect’ process continued for local reflections till the remaining clouds were too small (less than n/20). All the global and local reflections, as shown in Fig. 61.3a, were detected in 641.8 s in total; Fig. 61.3b shows the hierarchy of the reflections. It was found that the whole hierarchy of reflections was also symmetric to the plane of the global reflection. The symmetry hierarchy was applied to a RANSAC-based automatic rooftop modeling process to rectify the planar and spherical primitives [6]. As shown in Fig. 61.3c, a symmetry-guided rooftop model was created and attached to the ‘box’ model of the building. In summary, the pilot study preliminarily endorsed the feasibility and soundness of the proposed DFO approach.

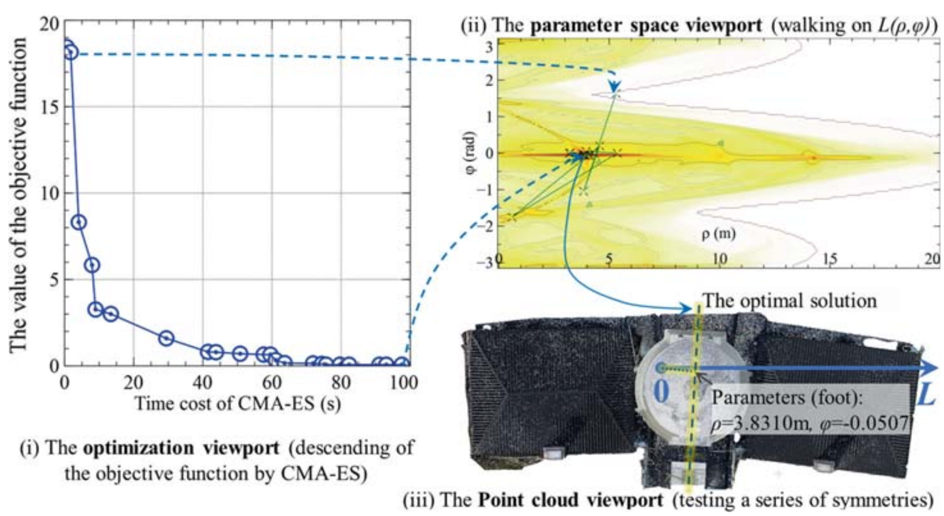

Fig. 61.2 Illustrations of ASD by the proposed DFO approach in three viewports

Table 61.1 A comparison of the results of detecting the global reflection symmetry

	Mitra and Pauly [16]	Cicconet et al. [18]	The DFO approach
Type	Voting-clustering	Voting-clustering	Parameter optim.
PCR[a]	90.7% (grid center)	9.77% (the best one)	**93.7%**
MSE[a](m^2)	0.091	19.164	**0.086**
Plane	$19.983X - Y = 78.033$	$7.914X - Y = 71.718$	$19.708X - Y = 75.596$
Correct?[a]	**Yes**	No (local only)	**Yes**
Time[a] (s)	140.7	837.7	**98.7**
Top view		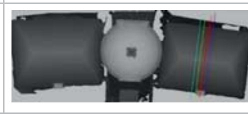	

[a]Best values in bold

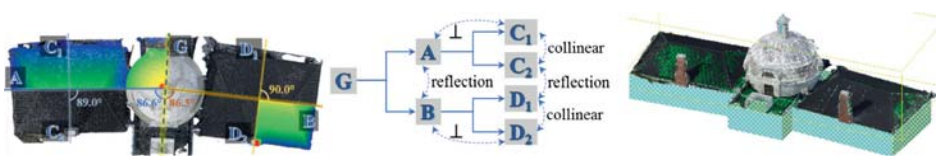

(a) The detected reflections (b) Symmetry hierarchy (c) A symmetry-guided model

Fig. 61.3 The hierarchy and an application of the detected symmetries

61.5 Conclusion

This paper presents a DFO approach for automatic ASD from 3D urban point clouds for creating CIM/BIM. In this approach, the symmetries and symmetry hierarchies can be formulated to nonlinear optimization problems, that concerns both the geometric symmetry condition and architectural style, and solved by DFO algorithms. The results of experiments on a pilot case, i.e., the best accuracy (both PCR and MSE) and efficiency (time cost)in detecting the global reflective symmetry, preliminarily confirmed its technological feasibility. The symmetry hierarchy was also validated in generating a symmetry-guided as-built rooftop model.

The contribution of this paper is twofold. First, the problem formulation in this approach exposes the problem of ASD from 3D urban point clouds to DFO algorithms and other mathematical methods. Secondly, The accurate and efficient DFO approach for ASD can be applied to the processing of large-scale 3D urban point clouds for enriching the urban semantics in CIM/BIM. Given the background of the boomingly available 3D urban point clouds and the demands of semantic CIM/BIM, the presented approach, and the enriched CIM/BIM at large, may enable various applications in heritage conservation, smart city development, architectural morphology, computational geometry, computer vision, and location-based services for a smart and resilient future.

Although the proposed DFO approach has many merits, the proposed approach relies on domain knowledge (architectural styles) in the formulation and only works with the clouds of uniformly distributed points. The experiments in this paper were also preliminary, e.g., focusing on reflections only. Possible future research directions include: (i) collecting, formulating, and compiling the typical architectural styles in urban areas, (ii) adopting, gauging, and fine-tuning state-of-the-art DFO algorithms, and (iii) integrating and applying the symmetries and symmetry hierarchy into popular CIM/BIM software platforms.

Acknowledgements This study was supported by a grant from the Hong Kong Research Grant Council (GRF HKU17201717) and two grants from The University of Hong Kong (201702159013, 201711159016).

References

1. Thompson, D.W.: On Growth and Form. Cambridge University Press, Cambridge (1961)
2. Fletcher, B., Fletcher, B.F.: A history of architecture on the comparative method, 5th edn. Agnew, & Co., London, Bradbury (1905)
3. Mitra, N.J., Pauly, M., Wand, M., Ceylan, D.: Symmetry in 3D geometry: extraction and applications. Comput. Graph. Forum **32**(6), 1–23 (2013). https://doi.org/10.1111/cgf.12010
4. Eastman, C.M., Eastman, C., Teicholz, P., Sacks, R.: BIM handbook: a guide to building information modeling for owners, managers, designers, engineers and contractors, 2nd edn. Wiley, Hoboken, NJ (2011)
5. Tang, P., Huber, D., Akinci, B., Lipman, R., Lytle, A.: Automatic reconstruction of as-built building information models from laser-scanned point clouds: a review of related techniques. Autom. Constr. **19**(7), 829–843 (2010). https://doi.org/10.1016/j.autcon.2010.06.007
6. Chen, K., Lu, W., Xue, F., Tang, P., Li, L.H.: Automatic building information model reconstruction in high-density urban areas: augmenting multi-source data with architectural knowledge. Autom. Constr. **93**, 22–34 (2018). https://doi.org/10.1016/j.autcon.2018.05.009
7. van Kaick, O., Zhang, H., Hamarneh, G., Cohen-Or, D.: A survey on shape correspondence. Comput. Graph. Forum **30**(6), 1681–1707 (2011). https://doi.org/10.1111/j.1467-8659.2011.01884.x
8. Conn, A.R., Scheinberg, K., Vicente, L.N.: Introduction to derivative-free optimization. SIAM, Philadelphia, PA (2009)
9. Rios, L.M., Sahinidis, N.V.: Derivative-free optimization: A review of algorithms and comparison of software implementations. J. Global Optim. **56**(3), 1247–1293 (2013). https://doi.org/10.1007/s10898-012-9951-y
10. Xue, F., Lu, W., Chen, K.: Automatic generation of semantically rich as-built building information models using 2D images: a derivative-free optimization approach. Comput. Aided Civil Infrastruct. Eng. in press (2018). https://doi.org/10.1111/mice.12378
11. Nicosia, G., Stracquadanio, G.: Generalized pattern search algorithm for peptide structure prediction. Biophys. J. **95**(10), 4988–4999 (2008). https://doi.org/10.1529/biophysj.107.124016
12. Hansen, N., Ostermeier, A.: Completely derandomized self-adaptation in evolution strategies. Evol. Comput. **9**(2), 159–195 (2001). https://doi.org/10.1162/106365601750190398
13. Xue, F., Lu, W., Chen, K., Zetkulic, A.: From 'semantic segmentation' to 'semantic registration': a derivative-free optimization-based approach for automatic generation of semantically rich as-built building information models (BIMs) from 3D point clouds. J. Comput. Civil Eng., under review (2018)
14. James, G.D.: The Representation Theory of the Symmetric Groups. Springer, New York (1978)
15. Mitra, N.J., Guibas, L.J., Pauly, M.: Partial and approximate symmetry detection for 3D geometry. ACM Trans. Graph. **25**(3), 560–568 (2006). https://doi.org/10.1145/1179352.1141924
16. Mitra, N.J., Pauly, M.: Symmetry for architectural design. In: Advances in Architectural Geometry. pp. 13–16. (2008). http://www.architecturalgeometry.org/aag08/aag08proceedings-papers_and_poster_abstracts.pdf
17. Kazhdan, M.: An approximate and efficient method for optimal rotation alignment of 3D models. IEEE Trans. Pattern Anal. Mach. Intell. **29**(7), 1221–1229 (2007). https://doi.org/10.1109/TPAMI.2007.1032
18. Cicconet, M., Birodkar, V., Lund, M., Werman, M., Geiger, D.: A convolutional approach to reflection symmetry. Pattern Recogn. Lett. **95**, 44–50 (2017). https://doi.org/10.1016/j.patrec.2017.03.022
19. Brown, C.M.: Inherent bias and noise in the Hough transform. IEEE Trans. Pattern Anal. Mach. Intell. **5**(5), 493–505 (1983). https://doi.org/10.1109/TPAMI.1983.4767428
20. Berner, A., Bokeloh, M., Wand, M., Schilling, A., Seidel, H. P.: A graph-based approach to symmetry detection. In: Volume Graphics, 40, pp. 1–8. ACM (2008). https://doi.org/10.2312/vg/vg-pbg08/001-008
21. Bokeloh, M., Berner, A., Wand, M., Seidel, H., Schilling, A.: Symmetry detection using feature lines. Comput. Graph. Forum **28**(2), 697–706 (2009). https://doi.org/10.1111/j.1467-8659.2009.01410.x
22. Andreopoulos, A., Tsotsos, J.K.: 50 years of object recognition: directions forward. Comput. Vis Image Underst. **117**(8), 827–891 (2013). https://doi.org/10.1016/j.cviu.2013.04.005
23. Monszpart, A., Mellado, N., Brostow, G.J., Mitra, N.J.: RAPter: rebuilding man-made scenes with regular arrangements of planes. ACM Trans. Graph. **34**(4), 103 (2015). https://doi.org/10.1145/2766995
24. Lipman, Y., Chen, X., Daubechies, I., Funkhouser, T.: Symmetry factored embedding and distance. ACM Trans. Graph. **29**(4), 103 (2010). https://doi.org/10.1145/1778765.1778840
25. Chertok, M., Keller, Y.: Spectral symmetry analysis. IEEE Trans. Pattern Anal. Mach. Intell. **32**(7), 1227–1238 (2010). https://doi.org/10.1109/TPAMI.2009.121
26. Raviv, D., Bronstein, A.M., Bronstein, M.M., Kimmel, R.: Full and partial sym-metries of non-rigid shapes. Int. J. Comput. Vis. **89**(1), 18–39 (2010). https://doi.org/10.1007/s11263-010-0320-3